A bacterial pathogen uses dimethylsulfoniopropionate as a cue to target heat-stressed corals

Melissa Garren, Kwangmin Son, Jean-Baptiste Raina, Roberto Rusconi, Filippo Menolascina, Orr H. Shapiro, Jessica Tout, David G. Bourne, Justin R. Seymour, Roman Stocker

Supplemental Material

I. Review of motility among coral pathogens

A review of current literature indicates that all known putative bacterial pathogens of reef-building corals are motile (Table S1). The commonality of this trait suggests that it may play an important role in the disease process.

Table S1. Overview of currently known putative coral pathogens.

Disease (Location)	Bacterium	Coral species infected	Motile	References
Bleaching (Mediterranean)	*Vibrio shiloi*	*Oculina patagonica*	yes	(Rosenberg & Falkovitz 2004)
Bleaching/lysis (Indian Ocean, Red Sea)	*Vibrio coralliilyticus*	*Pocillopora damicornis*	yes	(Meron *et al.* 2009)
White pox/White patch disease (Caribbean)	*Serratia marcescens*	*Acropora sp.*	yes	(Patterson *et al.* 2002)
Montipora white syndrome (Hawaii)	*Vibrio owensii*	*Montipora capitata*	yes	(Ushijima *et al.* 2012)
White plague (Red Sea)	*Thalassomonas loyana*	Multiple	yes	(Thompson *et al.* 2006)
White syndrome, Yellow Band (Caribbean)	*Vibrio carchariae* (synonym for *V. harveyi*)	*Acropora sp.*	yes	(Luna *et al.* 2010) (Cervino *et al.* 2008)
Yellow blotch/band (Caribbean)	*Vibrio alginolyticus* (+3 other *Vibrio* spp.)	*Montastraea sp.*	yes (all 4)	(Cervino *et al.* 2004)
Black Band (widespread)	Consortium including *Phormidium corallyticum* and *Beggiatoa*	Multiple	yes	(Richardson 1996)

II. Microfluidic experiments

i. Microinjector device for diffusive gradient chemotaxis assays

A 2.8 mm wide microchannel with a 400 μm wide injector (Fig. S1) was fabricated using soft lithography techniques described previously (Seymour *et al.* 2008) to establish diffusive gradients for chemotaxis assays. Briefly, the attractant was injected into the microchannel (Fig. S1; inlet B) as a 400 μm wide band equidistant from the channel side walls, while the cells were injected in the channel on either side of the band (Fig. S1; inlet A). The cells and attractant were flowed into the channel and then flow was stopped to allow the attractant to diffuse laterally and the cells to respond to the gradient. Dimethylsulfoniopropionate (DMSP·HCl; $C_5H_{10}SO_2$·HCl; TCI) was freshly prepared with FASW to make 15 μM, 45 μM, and 61 μM working solutions that closely corresponded to the amount of DMSP measured in the *P. damicornis* and *A. millepora* mucus samples. *A. millepora* was chosen as a second coral species to test because *V. coralliilyticus* is known to infect it as well (Sussman *et al.* 2009). These freshly prepared DMSP solutions, as well as *P. damicornis* mucus collected from Davies Reef (GBR; preserved at -80°C as described in section III and thawed on ice directly before experimental use; measured to contain 12-15 μM DMSP) and from corals maintained in the laboratory at MIT, *A. millepora* mucus from the GBR (containing 45-62 μM DMSP), and a FASW control were tested against overnight cultures of *V. coralliilyticus*.

The channel was loaded at moderate flow rates (2 μl per minute) to establish an initial experimental condition where the cells and the attractant were in discrete bands (Fig. S1B). To begin the experiment, the flow was stopped and the channel was imaged directly downstream of the end of the microinjector using phase-contrast video microscopy on a Nikon Ti microscope equipped with an Andor Neo CCD camera (6.5 μm/pixel), at 1 frame per second for 6 minutes. Five replicates of each experiment were conducted and the microchannel was flushed for 30 s with fresh cells and attractant between replicates. Flushing with FASW lasted 2 minutes in between different attractants. Each video was analyzed for cell positions using automated image segmentation software developed in house with MATLAB (MathWorks, Natick, MA). Background subtraction and cross-correlation functions were used to detect non-motile cells or other particles from the mucus, which were excluded from the cumulative cell distribution across the channel. Resulting time series of cell distributions are presented in the main text for *P. damicornis* (Fig. 1) and for *A. millepora* (Fig. S2).

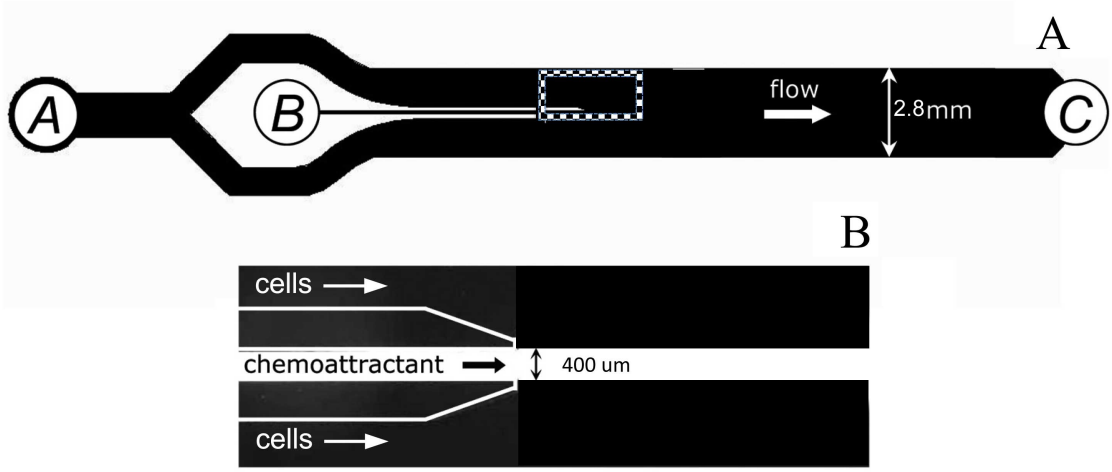

Figure S1. The microinjector chemotaxis assay. (**A**) A schematic of the entire channel where A is the inlet used to inject cells and B is the entrance point for the attractant into the microinjector (elongated structure on the right of B). C is the exit point of the channel. The dashed box shows where the camera field of view is focused during experiments to image half of the channel width. The channel is 100 µm deep. (**B**) A close-up picture of the microinjector (whose boundaries were marked by white lines for clarity) and of the central band it creates in the microchannel, visualized by addition of 100 µM fluorescein.

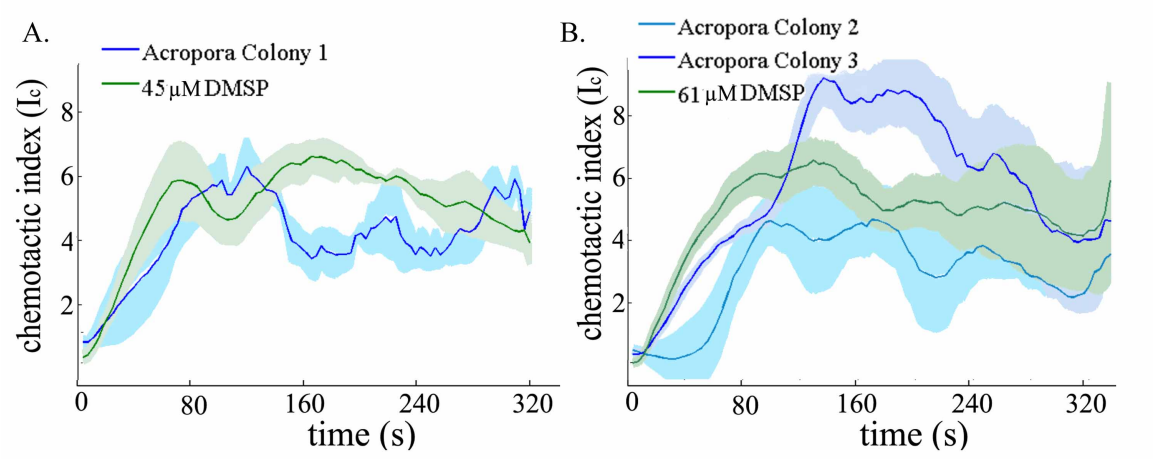

Figure S2. **The pathogen's chemotaxis is primarily triggered by DMSP in coral mucus.** The chemotactic response of *V. coralliilyticus* to a second coral species susceptible to infection, *A. millepora* (compare with Fig. 1 in the main text for *P. damicornis*). The mucus samples (blue lines) were run simultaneously with pure DMSP at the same concentration measured in each sample (green lines). All curves have been normalized by subtracting the mean value of the chemotactic index I_C over three FASW control runs, at each time point. The solid lines are the averages from three runs with each attractant and the shading denotes the standard error of the mean. Note how response levels were similar for whole coral mucus and DMSP alone, as found also for *P. damicornis*. (**A**) Colony 1 was measured to contain 45.3 ± 0.2 µM DMSP, and thus 45 µM DMSP (final concentration) diluted in FASW was run in parallel. (**B**) Colonies 2 and 3 were

measured to contain 60.7 ± 0.9 μM and 62.4 ± 2.0 μM DMSP, respectively, and were thus tested in parallel with 61 μM DMSP.

ii. 3-inlet device for single-cell tracking

To explore both the chemotactic and chemokinetic behaviors of *V. coralliilyticus* at the single cell scale, a 1 mm wide, 3-inlet channel (Fig. S3) was used to establish a transient diffusive gradient for long trajectory tracking. This channel configuration allowed a layer of FASW to be placed in between the cells and the attractant, where the latter was mucus, 100 μM DMSP or FASW (control). Compared to the microinjector (Fig. S1), the 3-inlet channel has the advantage of extending the duration of the gradient with the added layer of seawater between the cells and the attractant; thus, a longer window in which to visualize the dynamics of a single cell's behavioral response to the gradient is achieved. A 1:50 dilution of the overnight culture in FASW was injected in the upper inlet, FASW in the middle inlet, and the test attractant in the lower inlet. The channel was loaded at moderate flow rates (10 μl min^{-1}) to establish an initial condition where the three solutions were in three equal and discrete bands. To begin the experiment, the flow was stopped instantly by applying a pulse of negative pressure. Consequently, test attractants diffused across the width of the channel and the channel was imaged directly downstream of the inlet for 3 minutes in order to acquire long trajectories of individual bacteria. Darkfield video microscopy (15× objective, 60 frames/s) on a Nikon Ti microscope equipped with a Photron high-speed camera (SA-3, 17 μm/ pixel) was used for video acquisition. Five replicates of each experiment were conducted and the microchannel was flushed for 30 s with fresh cells, FASW, and attractant between replicates. Flushing with FASW lasted for 2 minutes in between different attractants.

Figure S3. This 3-inlet channel is 100 μm deep and has three 333 μm wide inlets that converge to form a 1 mm wide test channel with a single outlet at the end. The three inlets are used to create parallel bands of different solutions, as indicated in the figure. Bacteria responding to the diffusive gradients of the attractant are imaged immediately downstream of the junction between the three inlet microchannels.

A minimum of 50 trajectories were recorded per experiment and Fig. S4 shows 30 randomly selected trajectories from each test attractant. In the presence of diffusing DMSP or mucus exudates, cells swam towards the region of higher attractant concentration and the average swimming speed of the population, calculated from trajectories of individual bacteria and averaged over the entire width of the channel and over ~30 s after start of the experiments, increased 17% and 19% in the presence of DMSP and mucus exudates, respectively (Fig. S4). This increase in speed is a result of

chemokinesis – the process by which an organism changes its swimming speed in response to a change in the chemical concentration in its immediate environment.

However, this result does not reveal the full magnitude of the chemokinetic response because the change in speed was computed as an average over space and time, and cells experience different attractant concentrations at different positions and different times (since the gradient diffuses). To better identify the chemokinetic response, we sought to identify the relationship between the swimming speed and the mucus concentration, C (Fig. 3A in main text). To do so, we first computed the concentration of mucus exudates at each point across the channel for the entire time covered in the experiments by numerically solving the one-dimensional diffusion equation across the width of the microchannel in a domain having the same geometry as the experimental setup (Fig. S3) and with a diffusion coefficient D_C. To the best of our knowledge, the diffusion coefficient of DMSP is unknown. Therefore, we computed it using a correlation formula for the diffusivity of small molecules in water based on their molar volume (Wilke & Chang 1955), obtaining a value ($D_C = 10^{-9}$ m^2 s^{-1}) that is consistent with what has been used previously (Breckels *et al.* 2010). Trajectories were then used to compute instantaneous values of the swimming speed of single cells, V_S, and for each value of V_S we determined the instantaneous mucus concentration, C. This allowed us to bin instantaneous swimming speeds according to instantaneous concentrations (Fig. 3A in the main text), revealing the actual magnitude of the chemokinetic response (see main text).

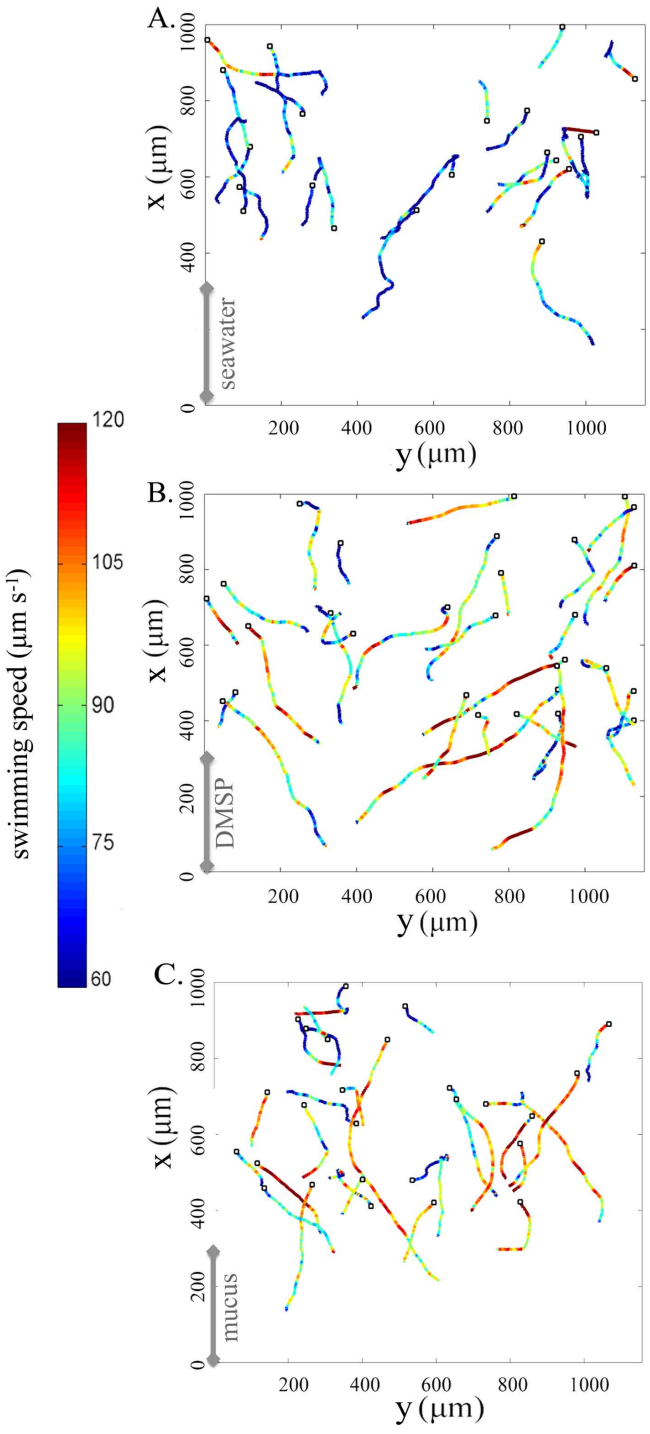

Figure S4. **Trajectories of individual bacteria** obtained in the 3-inlet microchannel (Fig. S3) in response to a diffusing, initially 333 µm wide layer (initial position identified by the gray bar along the *y* axis) of (**A**) FASW (control); (**B**) 100 µM DMSP; and (**C**) freshly collected coral mucus. The entire width of the channel (1 mm) is captured in the field of view. Open circle indicates starting points of each trajectory. Cells exposed to seawater maintain a relatively uniform, low speed, whereas cells exposed to mucus and DMSP considerably accelerate, a

behavior indicative of chemokinesis. Note that trajectories were acquired at different times: because the initial attractant layer diffused, local instantaneous concentrations varied for different trajectories. This time component is removed from the analysis, truly demonstrating chemokinesis, in an analysis of the swimming speed as a function of the instantaneous local concentration, shown in Fig. 3A of the main text. In all panels, x and y are the coordinates across and along the microchannel, respectively.

III. Chemotactic velocity (V_C)

The chemotactic velocity, V_C, is the mean drift velocity of a cell population in the direction of a gradient. In the microinjector experiments the chemoattractant gradient varied in space and time (Seymour *et al.* 2008), thus V_C also varied spatially and temporally (Fig. S5). We calculated V_C from the cell concentration profiles by numerically solving the bacterial transport equation (Keller & Segel 1971; Ahmed & Stocker 2008) and finding the parameters (chemotactic sensitivity and mean swimming speed) that best fitted the experimental cell distribution profiles, using a least squares method. The diffusivity D_B of the bacterial population was calculated from the dispersion of the cell distribution in the control experiments and was found to be 2×10^{-9} m^2 s^{-1}. This value is consistent with the random walk behavior of the bacteria, which leads to a diffusivity $D_B = V_S^2\,\tau_0/3$ (Berg 1993), which would give $V_S \sim 77$ µm s^{-1} with $\tau_0 \sim 1$ s (see section X).

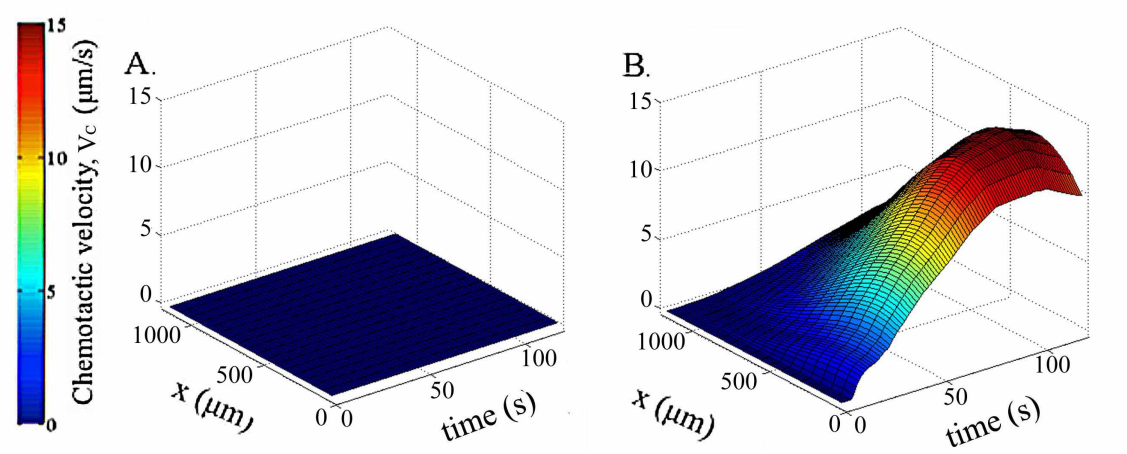

Figure S5. Chemotactic velocity, V_C, of *V. coralliilyticus*, computed from the microinjector chemotaxis experiment shown in Fig. 1 (see device in Fig. S1). (**A**) The control experiment where FASW was injected into the channel showed no chemotaxis. (**B**) Coral mucus injected into the channel as a band initially spanning $x = 0$ to 200 µm, injected at time zero, elicited strong chemotaxis. The vertical axis and the color bar both denote speed.

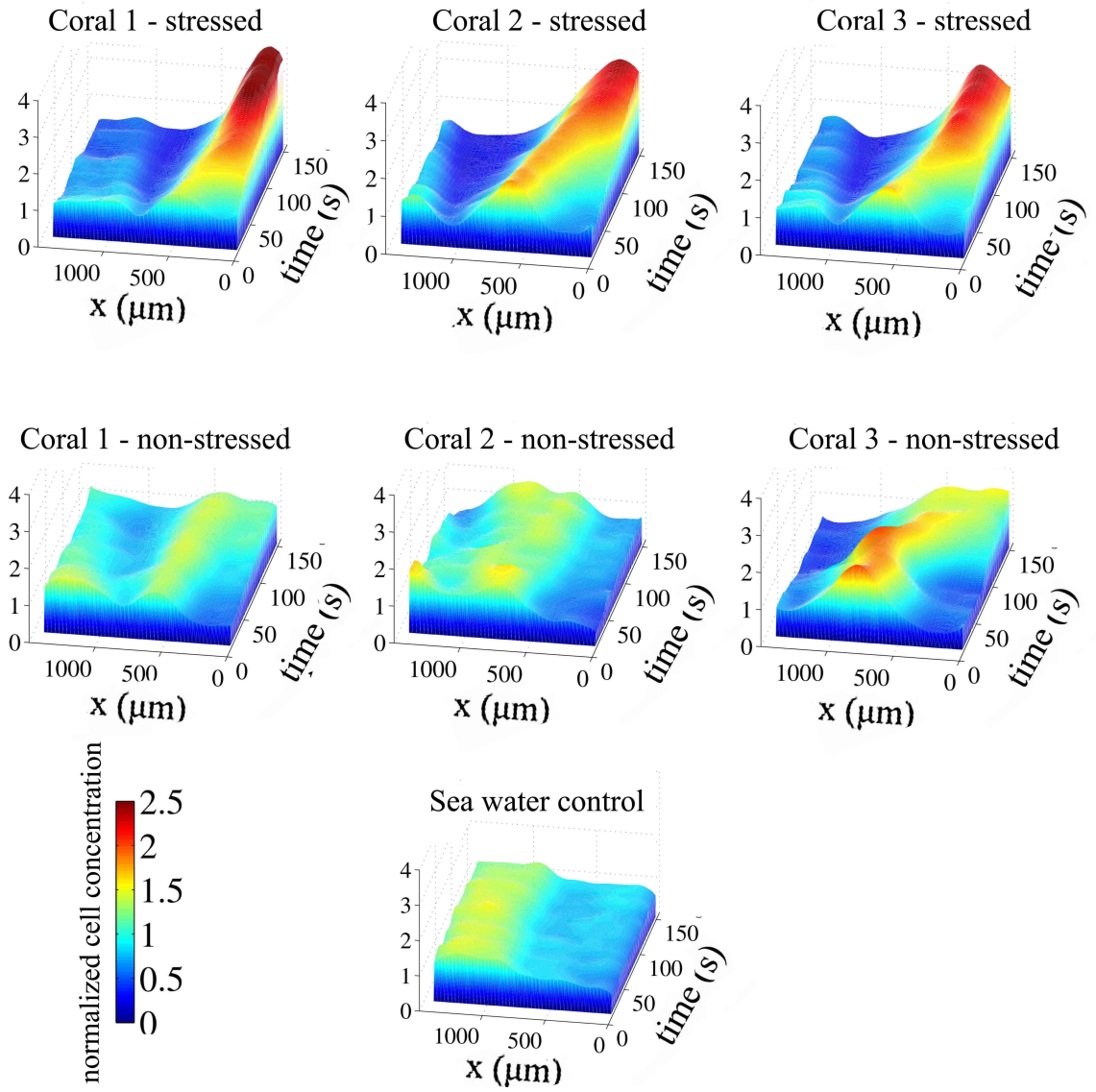

Figure S6. **Stressed corals elicit stronger chemotactic responses.** Results of individual chemotaxis assays performed in the microinjector channel (Fig. S1) for mucus collected from the Heron Island temperature-stress experiment. For each, the full time series of the spatial distribution of the pathogen population (vertical axis) across the width of the microfluidic channel, *x*, is shown (the experimental layout is the same as in Fig. 1C). Color and height both measure the local, instantaneous concentration of bacteria, normalized to a mean of 1, and the color bar is the same for all panels. 'Stressed' samples are from the final sampling time point where the fragments were at 31°C, whereas the control, 'non-stressed' samples are from the same donor colony but had been maintained at 22°C. Note how, despite some variability, stressed corals consistently induced a stronger chemotactic response compared to non-stressed corals.

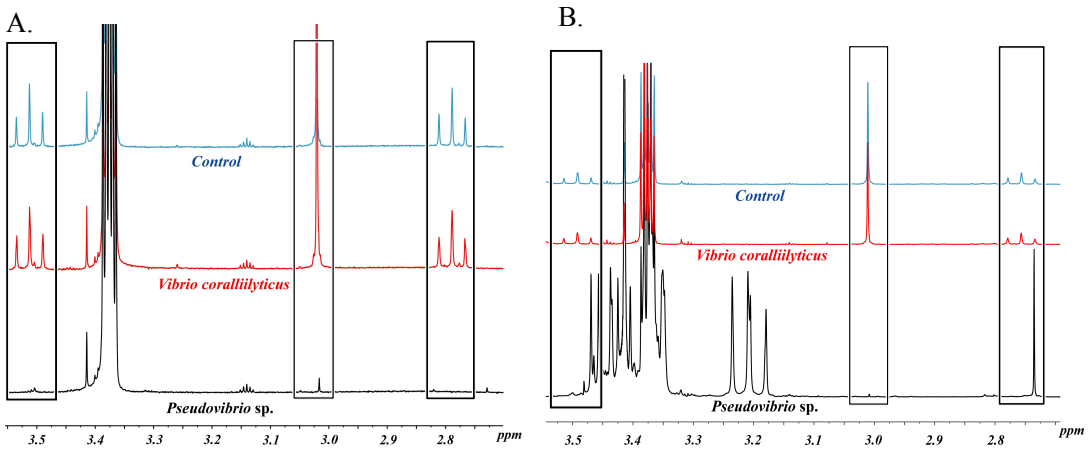

Figure S7. DMSP is not degraded by the pathogen during 6 day incubations. NMR traces after 6-day incubations in minimal media in which DMSP was (**A**) the sole carbon source and (**B**) the sole sulfur source. The "Control" traces refer to the growth medium where no bacteria were inoculated. The red and black traces show the results from inoculation with *V. coralliilyticus* and *Pseudovibrio* sp. (positive control), respectively. In both A and B, the DMSP peaks (black boxes) have the same intensity in the *V. coralliilyticus* treatment and in the no-bacteria, control, indicating that *V. coralliilyticus* did not consume DMSP, whereas they are depleted in the positive control. In the case of DMSP as a sole sulfur source (B), *Pseudovibrio* consumed the DMSP and other carbon sources in the medium and produced secondary metabolites (appearance of new peaks).

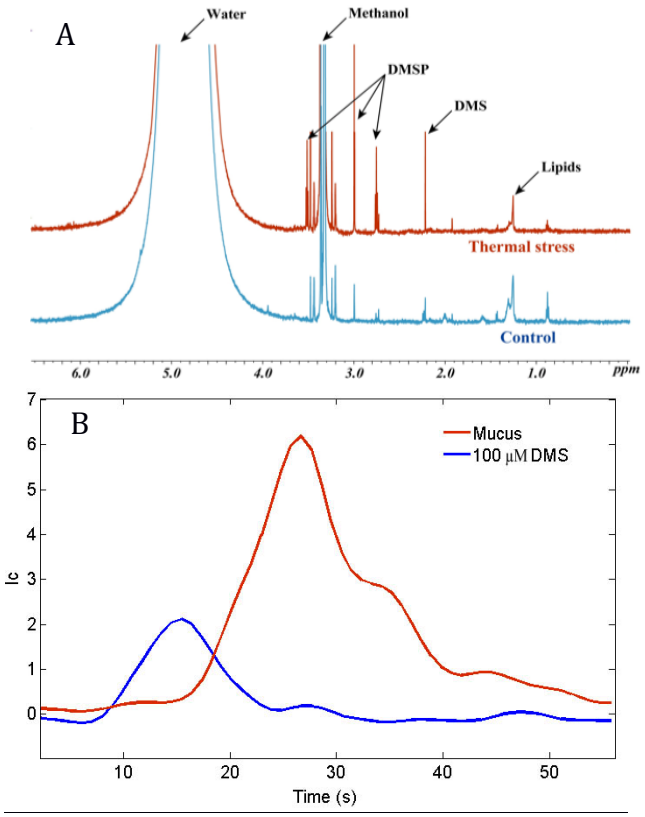

Figure S8. DMSP and DMS are the sole chemicals whose production greatly increased during heat stress. (**A**) Representative NMR spectra of *P. damicornis* mucus exposed to two different temperatures: 22°C (control) and 31°C (thermal stress). The chemical composition of coral mucus changed under thermal stress, with a dramatic increase in DMSP and its breakdown product DMS. The other natural constituents of coral mucus are largely unaffected by the rise in temperature. (**B**) Results from chemotactic assays demonstrating that *V. coralliilyticus* is only very weakly attracted to DMS in comparison to whole mucus. For reference, $I_C = 0$ corresponds to no chemotaxis and these experiments were performed in a 3-inlet channel 600 µm in width (Fig. S3).

IV. Steady gradient experiments in agarose microchannel

To test the chemokinetic response of *V. coralliilyticus* in a steady gradient, as a point of comparison to the unsteady, diffusive gradient experiments presented in Fig. 3A (see devices in Figs. S3, S4), a steady linear gradient of mucus solutes was created using a 2 mm wide agarose microchannel (Fig. S7A), fabricated by integrating a layer of agarose into a PDMS device as described previously(Ahmed *et al.* 2010). The agarose layer was made with 1.5% agarose in FASW and the overnight culture was diluted 1:3 in FASW to achieve an appropriate cell density for accurately tracking individual cells. Mucus solutes diffused through the agarose underneath the microchannel (Fig. S7B) and the gradient was allowed to establish in the channel by diffusion for a time of $L^2/(2D_C) \sim 33$ min (Ahmed *et al.* 2010) before cells were added to the test channel (here, L is the distance between the source and sink channels, $D \sim 10^{-9}$ m^2 s^{-1} is the diffusion coefficient of DMSP, and $L^2/(2D_C)$ is the characteristic diffusion time of the system). The entire width of the channel (Fig. S7a, x-direction) was imaged using a mosaic of 5 adjacent videos, each having a field of view of 296 μm × 395 μm, lasting 5 s and acquired at 10 frames/s. This was repeated for 20 different positions along the length of the channel (Fig. S7a, y-direction). From the 100 videos acquired, cell abundance and swimming speed were averaged over 150 μm wide bins across the width of the channel (see Fig. S7c), where the highest concentration of mucus is in the x = 1800–1950 μm bin and the lowest is in the x = 0-150 μm bin. The same experiment was repeated with a seawater control, using FASW in lieu of the mucus exudates.

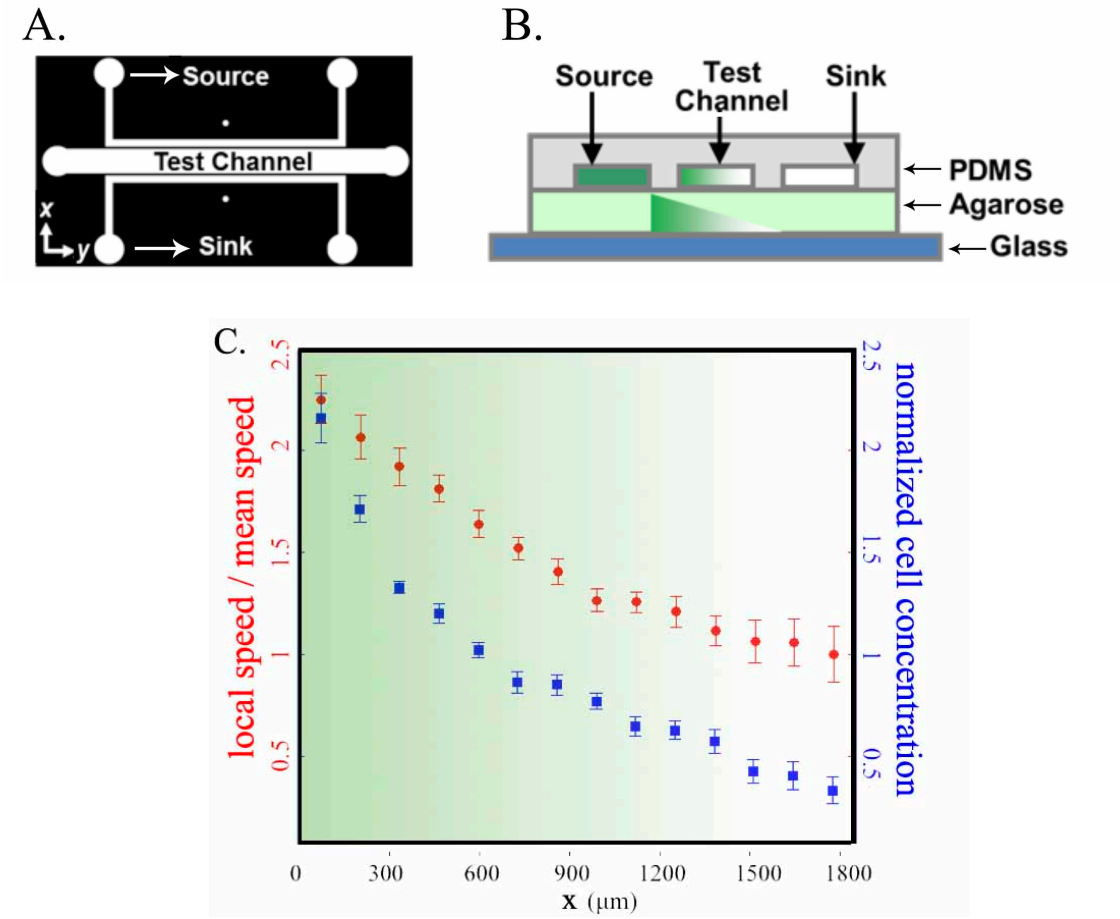

Figure S9. **(A)** Schematic planar view of the diffusion-based agarose microfluidic device showing source, sink and test channels. The space between the channels is 200 μm. **(B)** Schematic vertical cross section of the same device. By diffusing through the agarose and into the sink channel, mucus exudates flowing in the source channel form a linear gradient in the agarose slab, which in turn is transferred passively by diffusion into the test channel, where cells are contained. See ref. (Ahmed *et al.* 2010) for details on the layout, fabrication and operation of this microdevice. **(C)** Tracking of cells in a steady linear gradient of mucus solutes (illustrated schematically by the green shading) shows that pathogen accumulation (blue squares) in the region of highest mucus concentration is accompanied by an increase in the population-averaged swimming speed (red circles) with increasing mucus concentration. This is a result of chemokinesis. The relative swimming speed measures the increase in the average population swimming speed over the swimming speed in the lowest concentration region (x = 10 μm). The speed enhancement observed in this device (up to 120%) is greater than for the single-cell tracking experiment (Fig. 3A in the main text) because here the mean population speed was reduced by cells interacting with the agarose channel bottom, making percentage speed enhancements appear larger. Both experiments demonstrate that *V. coralliilyticus* exhibits strong chemokinesis.

V. Mathematical model of simultaneous chemotaxis and chemokinesis

We modeled the chemotaxis and chemokinesis of *V. coralliilyticus* by using an existing modeling framework for bacterial chemotaxis (BROWN & BERG 1974; Jackson 1987; Kiorboe & Jackson 2001), augmented by a concentration-dependent swimming speed that was based on our experimental observations (Fig. 3A). The model integrates the trajectories of individual bacteria as they swim in a chemoattractant gradient, within a domain that has the same width and boundary conditions as in the microfluidic setup used to quantify the chemotactic index of *V. coralliilyticus* responding to mucus or DMSP (Fig. S1). In this setup, the attractant gradient is transient, following the 'release' of an initial band of attractants. Thus, the spatiotemporal evolution of the attractant concentration at every position in the channel and every point in time was obtained by integrating the one-dimensional diffusion equation using MatLab (Mathworks, Natick, MA). The choice of the diffusivity, $D_C = 10^{-9}$ m^2 s^{-1}, was based on the diffusion coefficient of DMSP as described in section VI.ii. The model, largely based on *Escherichia coli,* as customary due to the lack of specific information for other species of bacteria, assumes that bacterial motion can be divided into runs (nearly straight swimming segments) and tumbles (reorientations in the swimming trajectory). When the bacterium experiences increasing attractant concentration, the probability of tumbling decreases (and vice versa), leading to positive chemotaxis.

The model is described in detail in ref. (Jackson 1987). Briefly, for each case we simulated 3,000 bacteria, initially distributed uniformly in the region of the channel not occupied by the central, 400-μm wide chemoattractant layer (Fig. S1). Bacteria in the simulations did not interact with each other. During a run a bacterium swims straight at a constant speed of 66 μm s^{-1} (the mean speed of a population measured in the absence of chemoattractants; see below for a modification to this rule in the case of chemokinesis), except for the effect of rotational diffusion, arising due to random collisions with water molecules and responsible for a random reorientation component. The value of the rotational diffusion coefficient, $D_R = 0.035$ rad^2 s^{-1}, was based on a resistive force model that accounted for both the cell body (3.2 μm long and 1.2 μm wide) and the helical flagellum (contour length 4.6 μm, pitch 1.5 μm) of the bacteria, as done in ref. (Marcos *et al.* 2012). During every time step of the integration, Δt, a new swimming direction was chosen at random (tumble) if a randomly generated number (between 0 and 1) was smaller than the probability of tumbling P_t, given by

$$P_t = \frac{\Delta t}{\tau}.$$

Here, τ is the mean run time, given by

$$\ln \tau = \ln \tau_o + \alpha \overline{\frac{\mathrm{d}P_b}{\mathrm{d}t}},$$

$$\overline{\frac{\mathrm{d}P_b}{\mathrm{d}t}} = \frac{1}{T_m}\int_{-\infty}^{t} \frac{\mathrm{d}P_b}{\mathrm{d}t'} \exp\left[\frac{t' - t}{T_m}\right] \mathrm{d}t',$$

$$\frac{\mathrm{d}P_b}{\mathrm{d}t} = \frac{K_D}{(K_D + C)^2}\frac{\mathrm{d}C}{\mathrm{d}t},$$

where T_m = 1 s is a time constant of the bacterial system (a memory term), τ_o= 1 s is the mean run time (tumbling interval) in the absence of concentration gradients, *C* is the mucus concentration relative to the maximum mucus concentration initially released in the microchannel, $\alpha = 660$ s is a system time constant (amplification factor), P_b is the fraction of surface receptors bound by the substrate, $\overline{dP_b/dt}$ is a weighted rate of change of P_b, and K_D= 20 is the half-saturation constant of the surface receptor binding to the attractant (also relative to the maximum initial attractant concentration). The choice of parameter values is in line with previous models (Jackson 1987; Kiorboe & Jackson 2001), with the exception of K_D, for which a value was chosen that produced a chemotactic index of comparable magnitude to the experimentally observed one (Fig. 2A in the main text). The model, then, allowed for the comparison of the chemotactic index in the presence and absence of chemokinesis.

VI. Blast search for DMSP degradation genes

Given our finding that DMSP is a strong chemoattractant for *V. coralliilyticus* even though the pathogen was unable to metabolize it, we further investigated the presence of genes involved in DMSP transformation in the *V. coralliilyticus* genome. While uptake of DMSP is known to be mediated by transporters in the BCCT and ABC families (for example C9NQ29_9VIBR and C9NQK8_9VIBR in *V. coralliilyticus*; *(Sun et al. 2012)*), two main biochemical routes have been found in bacteria degrading DMSP (Moran *et al.* 2012): (a) the *dmdA* gene allows DMSP demethylation and (b) *ddd* genes mediate the conversion of DMSP to dimethylsulfide (DMS). To cover a broader range of possibilities, we performed a blast search for DMSP degradation genes where we considered all of the confirmed sequences available in the literature for each gene involved in DMSP degradation (Howard *et al.* 2006; Todd *et al.* 2007; Howard *et al.* 2008; Todd *et al.* 2009; Curson *et al.* 2011; Todd *et al.* 2011; Todd *et al.* 2012). Table S2 lists, for each gene, the species whose genomic sequences have been considered in this analysis.

In order to assess the potential ability of *V. coralliilyticus* to metabolize DMSP we looked for statistically significant alignments (blast v. 2.2.27+) of all the sequences for each gene in Table S2 to any genome available for *V. coralliilyticus* in NCBI's nucleotide collection database (*V. coralliilyticus P1, V. coralliilyticus YB1, V. coralliilyticus LMG 20984, V. coralliilyticus ATCC BAA-450, V. coralliilyticus CAIM 616*). In line with our results from the metabolic experiments, none of these queries returned alignments that would suggest any of the probed genes were present in *V. coralliilyticus* (best matches had <1% coverage and alignment scores <40). Similar results were obtained by extending the same alignment procedure to all species in the genus *Vibrio*. Together these results suggest that *V. coralliilyticus* may not have evolved mechanisms to metabolize DMSP. Therefore, chemotaxis towards this compound has most likely evolved for purposes other than metabolism in this organism.

Table S2. DMSP degradation genes blasted against *V. coralliilyticus* genome.

DMSP degradation gene	Sequence source
dddD	*Marinomonas* sp. MWYL1 *Burkholderia cepacia* AMMD *Rhizobium* sp. NGR234 *Marinomonas* sp. MED121 *Marinobacter* sp. ELB17 Marine gammaproteobacterium HTCC2207 *Hoeflea phototrophica* DFL-43 *Sagittula stellata* E-37 *Burkholderia phymatum* STM815 *Burkholderia ambifaria* MC40-6 *Dinoroseobacter shibae* DFL 12 *Ruegeria pomeroyi* DSS-3
dddL	*Dinoroseobacter shibae* DFL 12 *Fulvimarina pelagi* HTCC2506 *Loktanella vestfoldensis* SKA53 *Oceanicola batsensis* HTCC2597 *Rhodobacter sphaeroides* *Rhodobacterales bacterium* HTCC2654 *Stappia aggregata* IAM 12614 *Sulfitobacter* sp. EE-36
dddP	*Aspergillus oryzae* RIB40 *Ruegeria pomeroyi* DSS-3 *Roseobacter litoralis* Och 149 *Oceanicola granulosus* HTCC2516 *Phaeobacter gallaeciensis* 2.10 Roseovarius sp. TM1035 Rhodobacterales bacterium HTCC2255 *Roseobacter denitrificans* OCh 114 *Roseovarius* sp. 217 *Jannaschia* sp. CCS1 *Phaeobacter gallaeciensis* BS107 *Rhodobacterales bacterium* HTCC2150 *Roseobacter* sp. SK209-2-6 *Roseovarius nubinhibens* ISM *Silicibacter* sp. TM1040
dddQ	*Ruegeria pomeroyi* DSS-3 *Roseovarius nubinhibens* ISM

dddW	*Ruegeria pomeroyi* DSS-3 *Roseobacter* sp. MED193
dddY	*Shewanella baltica* OS155 *Shewanella piezotolerans* WP3
dmdA	*Roseovarius nubinhibens* ISM *Dinoroseobacter shibae* DFL 12 *Jannaschia* sp. CCS1 *Silicibacter* sp. TM1040 Alphaproteobacterium BAL199 Rhodobacterales bacterium HTCC2150 *Pelagibacter ubique* HTCC1062 *Roseovarius* sp. TM1035 Marine gammaproteobacterium HTCC2080 *Roseobacter* sp. MED193

Supplementary references

Ahmed, T., Shimizu, T.S. & Stocker, R. (2010). Bacterial Chemotaxis in Linear and Nonlinear Steady Microfluidic Gradients. *Nano Letters*, 10, 3379-3385.

Ahmed, T. & Stocker, R. (2008). Experimental Verification of the Behavioral Foundation of Bacterial Transport Parameters Using Microfluidics. *Biophysical Journal*, 95, 4481-4493.

Berg, H. (1993). *Random walks in biology*. Princeton University Press.

Breckels, M.N., Boakes, D.E., Codling, E.A., Malin, G., Archer, S.D. & Steinke, M. (2010). Modelling the concentration of exuded dimethylsulphoniopropionate (DMSP) in the boundary layer surrounding phytoplankton cells. *Journal of Plankton Research*, 32, 253-257.

Brown, D.A. & Berg, H.C. (1974). Temporal simulation of chemotaxis in *Escherichia coli* . *PNAS*, 1388–1392.

Cervino, J.M., Hayes, R.L., Polson, S.W., Polson, S.C., Goreau, T.J., Martinez, R.J. *et al.* (2004). Relationship of Vibrio species infection and elevated temperatures to yellow blotch/band disease in Caribbean corals. *Applied and Environmental Microbiology*, 70, 6855-6864.

Cervino, J.M., Thompson, F.L., Gomez-Gil, B., Lorence, E.A., Goreau, T.J., Hayes, R.L. *et al.* (2008). The Vibrio core group induces yellow band disease in Caribbean and Indo-Pacific reef-building corals. *Journal of Applied Microbiology*, 105, 1658-1671.

Curson, A.R.J., Sullivan, M.J., Todd, J.D. & Johnston, A.W.B. (2011). DddY, a periplasmic dimethylsulfoniopropionate lyase found in taxonomically diverse species of Proteobacteria. *Isme Journal*, 5, 1191-1200.

Howard, E.C., Henriksen, J.R., Buchan, A., Reisch, C.R., Buergmann, H., Welsh, R. *et al.* (2006). Bacterial taxa that limit sulfur flux from the ocean. *Science*, 314, 649-652.

Howard, E.C., Sun, S.L., Biers, E.J. & Moran, M.A. (2008). Abundant and diverse bacteria involved in DMSP degradation in marine surface waters. *Environmental Microbiology*, 10, 2397-2410.

Jackson, G.A. (1987). Simulating chemosensory response of marine microorganisms. Limnology & Oceanography, pp. 1253–1266

Keller, E.F. & Segel, L.A. (1971). Model for chemotaxis. *Journal of Theoretical Biology*, 30, 225-&.

Kiorboe, T. & Jackson, G.A. (2001). Marine snow, organic solute plumes, and optimal chemosensory behavior of bacteria. *Limnology and Oceanography*, 46, 1309-1318.

Luna, G.M., Bongiorni, L., Gili, C., Biavasco, F. & Danovaro, R. (2010). Vibrio harveyi as a causative agent of the White Syndrome in tropical stony corals. *Environmental Microbiology Reports*, 2, 120-127.

Marcos, Fu, H.C., Powers, T.R. & Stocker, R. (2012). Bacterial rheotaxis. *Proceedings of the National Academy of Sciences of the United States of America*, 109, 4780-4785.

Meron, D., Efrony, R., Johnson, W.R., Schaefer, A.L., Morris, P.J., Rosenberg, E. *et al.* (2009). Role of Flagella in Virulence of the Coral Pathogen Vibrio coralliilyticus. *Applied and Environmental Microbiology*, 75, 5704-5707.

Moran, M.A., Reisch, C.R., Kiene, R.P. & Whitman, W.B. (2012). Genomic Insights into Bacterial DMSP Transformations. *Annual Review of Marine Science, Vol 4*, 4.

Patterson, K.L., Porter, J.W., Ritchie, K.E., Polson, S.W., Mueller, E., Peters, E.C. *et al.* (2002). The etiology of white pox, a lethal disease of the Caribbean elkhorn coral, Acropora palmata. *Proceedings of the National Academy of Sciences of the United States of America*, 99, 8725-8730.

Richardson, L.L. (1996). Horizontal and vertical migration patterns of Phormidium corallyticum and Beggiatoa spp associated with black-band disease of corals. *Microbial Ecology*, 32, 323-335.

Rosenberg, E. & Falkovitz, L. (2004). The Vibrio shiloi/Oculina patagonica model system of coral bleaching. *Annual Review of Microbiology*, 58, 143-159.

Seymour, J.R., Ahmed, T., Marcos & Stocker, R. (2008). A microfluidic chemotaxis assay to study microbial behavior in diffusing nutrient patches. *Limnology and Oceanography-Methods*, 6, 477-488.

Sun, L., Curson, A.R.J., Todd, J.D. & Johnston, A.W.B. (2012). Diversity of DMSP transport in marine bacteria, revealed by genetic analyses. *Biogeochemistry*, 110, 121-130.

Sussman, M., Mieog, J.C., Doyle, J., Victor, S., Willis, B.L. & Bourne, D.G. (2009). Vibrio Zinc-Metalloprotease Causes Photoinactivation of Coral Endosymbionts and Coral Tissue Lesions. *Plos One*, 4.

Thompson, F.L., Barash, Y., Sawabe, T., Sharon, G., Swings, J. & Rosenberg, E. (2006). Thalassomonas loyana sp nov, a causative agent of the white plague-like disease of corals on the Eilat coral reef. *International Journal of Systematic and Evolutionary Microbiology*, 56, 365-368.

Todd, J.D., Curson, A.R.J., Dupont, C.L., Nicholson, P. & Johnston, A.W.B. (2009). The dddP gene, encoding a novel enzyme that converts dimethylsulfoniopropionate into dimethyl sulfide, is widespread in ocean metagenomes and marine bacteria and also occurs in some Ascomycete fungi. *Environmental Microbiology*, 11, 1376-1385.

Todd, J.D., Curson, A.R.J., Kirkwood, M., Sullivan, M.J., Green, R.T. & Johnston, A.W.B. (2011). DddQ, a novel, cupin-containing, dimethylsulfoniopropionate lyase in marine roseobacters and in uncultured marine bacteria. *Environmental Microbiology*, 13, 427-438.

Todd, J.D., Kirkwood, M., Newton-Payne, S. & Johnston, A.W.B. (2012). DddW, a third DMSP lyase in a model Roseobacter marine bacterium, Ruegeria pomeroyi DSS-3. *Isme Journal*, 6, 223-226.

Todd, J.D., Rogers, R., Li, Y.G., Wexler, M., Bond, P.L., Sun, L. *et al.* (2007). Structural and regulatory genes required to make the gas dimethyl sulfide in bacteria. *Science*, 315, 666-669.

Ushijima, B., Smith, A., Aeby, G.S. & Callahan, S.M. (2012). Vibrio owensii Induces the Tissue Loss Disease Montipora White Syndrome in the Hawaiian Reef Coral Montipora capitata. *Plos One*, 7.

Wilke, C.R. & Chang, P. (1955). Correlation of diffusion coefficients in dilute solutions. *Aiche Journal*, 1, 264-270.

Movie caption

Movie S1. Coral mucus attracts the pathogen *V. coralliilyticus*. This movie excerpt is from the experiment displayed in Fig. 1. These 15 seconds of video are seconds 100-115 in the experiment, and are the same frames used to create the trajectory image displayed in Fig. 1B. Mucus was initially injected on the right-hand side of the channel and *V. coralliilyticus* cells on the left-hand side.